J Nanostruct 15(3): 1475-1492, Summer 2025

RESEARCH PAPER

Green Synthesis and Synergistic Anticancer Activity of Mycogenic Selenium Nanoparticles Using *Exserohilum rostratum*

Ahmad K. Hachim [1,2,3] *, ***Basil A. Abbas*** [4], ***Monia El Bour*** [2]

[1] *University of Tunis El-Manar, Faculty of Sciences, El Manar II - 2092, Tunis, Tunisia*

[2] *University of Carthage, National Institute of Marine Sciences and Technology (INSTM), Tunis, Tunisia*

[3] *General Directorate for Education, Basrah, Iraq*

[4] *Department of Microbiology, Faculty of Veterinary Medicine, University of Basra, Basrah, Iraq*

ARTICLE INFO

Article History:
Received 19 April 2025
Accepted 24 June 2025
Published 01 July 2025

Keywords:
Antioxidant activity
Cytotoxicity
Endophytic fungi
Mycofabrication
Selenium nanoparticles (SeNPs)

ABSTRACT

The increasing applications of selenium nanoparticles (SeNPs) in biomedical and industrial fields have drawn attention to eco-friendly synthesis methods. This study presents a green approach for SeNP production utilizing the endophytic fungus *Exserohilum rostratum*. The fungus-derived cell-free filtrate played a dual role as both a reducing and stabilizing medium, promoting the development of stable, spherical SeNPs. FESEM imaging revealed nanoparticle sizes ranging from 8.17 to 19.61 nm, averaging 14.26 nm in diameter. Antioxidant capacity was assessed via the DPPH assay, showing concentration-dependent scavenging efficiency ranging from 23.93 ± 4.74% to 83.3 ± 1.74%. Cytotoxicity evaluations using MTT assays showed selective inhibitory effects on cancer cell lines MCF7 and PC3, with IC_{50} values of 134.67 ± 1.98 µg/mL and 84.0 ± 2.06 µg/mL, respectively. In contrast, normal HBL-100 cells exhibited a significantly higher IC_{50} (405.9 ± 23.7 µg/mL), indicating reduced toxicity. Notably, co-administration with doxorubicin led to enhanced anticancer activity, decreasing the IC_{50} values to 50.55 µg/mL (MCF7) and 22.17 µg/mL (PC3), suggesting a synergistic interaction. These findings indicate that fungal-mediated SeNPs offer a promising, biocompatible nanomaterial with potential for enhanced anticancer therapy.

How to cite this article
Hachim A., El Bour M., Abbas B. Green Synthesis and Synergistic Anticancer Activity of Mycogenic Selenium Nanoparticles Using Exserohilum rostratum. J Nanostruct, 2025; 15(3):1475-1492. DOI: 10.22052/JNS.2025.03.061

INTRODUCTION

Cancer's pathogenic complexity is attributed to various processes, including different genetic anomalies, epigenetic alterations, interactions within the tumor microenvironment, and immune system evasion [1]. Even within the same tissue type, each tumor may have a unique molecular profile, resulting in a wide range of therapy responses. Furthermore, cancer cells can adapt and develop resistance to treatments over time, further complicating care [2]. This complicated pathophysiology challenges accurate diagnosis. Treatment is particularly complicated by the need for personalized therapy procedures that take into consideration individual tumor biology, potential drug resistance mechanisms, and patient-specific

* *Corresponding Author Email: hachimahmad31@gmail.com*

characteristics [3,4]. To treat cancer, healthcare professionals use a variety of therapies, such as surgery, chemotherapeutic drugs, hormone therapy, and radiation. Nonetheless, these treatments are often ineffectual because the majority of cases are diagnosed at advanced stages, indicating potential limitations in their administration [5,6]. Androgen deprivation is one approach used to treat metastatic prostate cancer [3]. This medication leads to toxicity with undesirable effects, including cardiovascular diseases, low bone density, metabolic modifications, and cognitive and sexual impairments [7,8]. Almost 70% of women diagnosed with breast cancer exhibit estrogen receptor positivity, and the preferred treatment is tamoxifen [5]. This treatment may have unintended consequences, which include the possibility of acquiring an alternative carcinoma, like cancer of the endometrium, as well as significant cerebrovascular difficulties, embolism in the lungs, and coronary vein thromboembolism [9]. Along with the potential negative consequences, another obstacle to cancer therapy is the establishment of mechanisms that confer resistance to chemotherapy and radiation, which result in the inefficiency of the administered treatments [1, 10]. As a result, the most successful tactics for combating cancer are to implement programs for early detection and advanced research to discover novel therapy agents [11]. To accelerate this discovery pipeline, microfluidic devices driven by surfaceacousticwave streaming can form uniform multicellular tumour spheroids within minutes, yielding highly realistic invitro models for nanoparticle testing [11].

Nanotechnology has profoundly altered medical research and therapy choices during the last three decades [12]. Nanoparticles have proven effective as pharmaceutical carriers, successfully delivering therapeutic substances [13]. Equally important, porousgradient microfluidic chips permit realtime chemotaxis assays and could be adapted to trace SeNPguided cancercell migration with singlecell precision [68]. Selenium, an essential trace element, has pharmacological activities, and the selenium nanoparticles (SeNPs) retain their biological properties in nanoparticle formulations for medicinal applications. [14]. Selenium possesses significant medicinal and pharmaceutical properties due to its integration into selenoproteins, which are missing in other metal nanoparticles. Selenoproteins are essential for the activation of kinases, phosphatases, and regulatory genes, including NF-κB, through the oxidation of thiols in signaling proteins [15, 16].

Recent research studies have reported the therapeutic potential of cancer drug delivery by biosynthesized SeNPs. SeNPs are synthesized in various ways, including biogenic, chemical, and physical synthesis processes. However, biogenic synthesis of SeNPs is relatively more stable than those synthesized through chemical and physical processes due to the presence of biomolecular coatings [17, 18]. These biomolecular coatings are the aggregation of biosynthesized SeNPs. Non-biogenic synthesis processes, on the other hand, necessitate hazardous chemicals, operate at pH levels, and require high temperatures [5], thus making the SeNPs dangerous for human consumption [19]. Therefore, biogenic SeNPs are safer for therapeutic applications [20]. Moreover, Se-NPs can potentially activate T cells of the immune system and thereby modulate tumor-associated macrophages. Therefore, SeNPs can be regarded as an immunomodulatory agent and can thereby be used in pathogen-targeted therapies for infectious diseases and cancer immunotherapy [15,21].

In the past few years, fungi, including endophytic fungi, have been at the forefront of advancements in nanotechnology. Fungal species are increasingly utilized in green synthesis methods for nanoparticles due to their natural enzymatic pathways, which can efficiently produce metallic nanoparticles with reduced toxicity [22,23]. These nanoparticles possess extensive applications in medical care, agriculture, and environmental science, ranging from targeted drug delivery to wastewater treatment [24,25]. Beyond oncology, nanoenabled formulations have already boosted pediculicidal efficacy by coupling ironoxide nanoparticles with botanical extracts, underlining the breadth of therapeutic opportunities for biofabricated nanomaterials [69]. Endophytic fungi also contribute to nanoproduct innovation by synthesizing nanomaterials that mimic or enhance their natural bioactivity [10,26]. Moreover, their sustainable synthesis processes align with the growing demand for environmentally friendly technologies, making fungi essential players in both natural product development and nanotechnology. Recent investigations have emphasized the potential therapeutic applications

of mycosynthesized selenium nanoparticles fabricated from several fungal species, revealing their anti-cancer and antioxidant properties [23,27,28,29,30].

The endophytic fungus *Exserohilum rostratum* produces physiologically active secondary metabolites and extracellular enzymes, attracting scientific attention. Bioactive Monocerin, Annularins A–J, and Rostratins A–D are antibacterial, antioxidant, and cytoprotective. Monocerin increases HUVEC proliferation and prevents senescence without cytotoxicity, suggesting therapeutic potential [31]. Besides its metabolite profile, *E. rostratum* has DNase, lipase, amylase, and cellulase activity and can decolorize Congo Red and Crystal Violet, rendering it advantageous in bioremediation and enzyme-based industrial applications [32].

E. rostratum is a promising biological system for the environmentally sustainable production of metal and metalloid nanoparticles owing to these attributes. We show for the first time that *E. rostratum* can biosynthesize selenium nanoparticles (SeNPs) utilizing its cell-free filtrate in an environmentally friendly, straightforward, and effective manner. This filtrate aids in the production of stable colloidal SeNPs by reducing and stabilizing them. The myco-synthesized SeNPs underwent comprehensive characterization through UV–Vis, FTIR, XRD, FESEM, EDX, and AFM techniques. The biological importance of fungal-mediated SeNP production was evaluated by assessing their antioxidant, cytotoxic, anticancer, and synergistic effects with conventional chemotherapy.

MATERIALS AND METHODS

Endophytic fungi, isolation process

Exserohilum rostratum is an endophytic fungus purified from stems of *Schoenoplectiella articulata* plants of the Cyperaceae family. The plant stem samples were collected from the native regions of the Basra Basin, southern Iraq, in 2024, following the steps outlined by Greenfield et al. [33]. The plant stems were sectioned into 5 cm fragments and gently rinsed under running tap water for 10 minutes, followed by washing in sterilized distilled water. The plant stem fragments were surface-disinfected using 70% alcohol for 5 minutes, followed by a 2-minute treatment with a 5% sodium hypochlorite solution, and then cleaned using 90% alcohol for 1 minute and then immersed in 10% $NaHCO_3$ to eradicate all the fungus contamination on the plant stem. The plant stem fragments were washed well using sterile distilled water three times. The fragments were exposed to air under sterilized conditions and subsequently transferred to sterile potato dextrose agar (PDA) enriched with tetracycline (20 μg/ml) to prevent bacterial growth. Bacterial growth. The plates had been incubated at 28 °*C* and maintained for 14 days to allow the development of the endophytic fungus to obtain the efficient isolation of the pure cultures on the PDA.

Identification of endophytic fungi isolation

A fungus culture was cultivated as an axenic culture on PDA culture plates and microscopically analyzed to determine its morphological characteristics, as described in the taxonomic descriptions by Ellis [34], Domsch et al. [35], and Watanabe [36]. The purified endophytic fungus culture was identified using molecular analyses. The purification of the deoxyribonucleic acid (DNA) has been conducted by the DNA purification kit Gene Jet Plant genomic (Thermo). During the purification process, the primers ITS1 (5'-TCC GTA GGT GAA CCT CGG G-3') and ITS4 (5'-TCC TCC GCT TAT TGA TAT GC-3') were employed. After a successful PCR amplification technique, sequences were transmitted to the Macrogen biotechnology company, and the product was purified to get ready for sequencing. Using the Basic Local Alignment Search Tool (BLAST), the sequence findings were compared to NCBI gene sequences to identify the closest match for the fungal isolate. MEGA X performed the Neighbor Joining (NJ) tree technique to create the phylogenetic tree.

Endophytic fungus culture conditions and bio-synthesis of Selenium Nanoparticles

This study utilized the endophyte species *Exserohilum rostratum* Basra_A15, isolated from *Schoenoplectiella articulata*, for the fabrication of selenium nanoparticles. The fungal culture was prepared using the method presented by Amin et al. [37], with minor changes. Briefly, 250 mL flasks with 100 mL of sterilized potato dextrose broth (PDB), adjusted to a pH of 5.6, were inoculated with a 7 mm disc from a 7-day-old fungus colony. The flasks with the culture were incubated in a static state at 28°C for two weeks. Subsequently, after the fermentation period, the fungal biomass was separated from the culture medium through

centrifugation at 6000 rpm for 10 minutes at a temperature of 10°C. The recovered mycelia were rinsed several times using distilled water to eliminate the remaining substance components in the biomass. The extracellular fabrication of nano selenium was conducted by suspending 10 g of wet fungal biomass in 100 mL of sterilized deionized water in Erlenmeyer flasks. The suspension was stirred in a water bath at 120 rpm for 72 hrs at 28°C. After incubation, the resulting solution was processed by filtration through filter paper (Whatman No. 1) to obtain the fungal cell-free filtrate (FCF). The mycosynthesis of SeNPs was then initiated by incubating the FCF with aqueous sodium selenite (Na_2SeO_3) at a final concentration of 1 mM, in the dark at room temperature. Control flasks contained sodium-selenite-free cell filtrate. Triplicate flasks were used for both untreated and treated FCF.

Detection, Purification, and Characterization of Mycosynthesis-SeNPs

Following a 24-hour duration, the hue of the free cell filtrate transitioned from a light yellow to a striking red, thereby validating Mycofabrication SeNPs. The purification of the mycosynthesized SeNPs was conducted through centrifugation, executed for ten minutes, with three repetitions of 10,000 rpm, utilizing double-distilled water. The particles were subjected to refrigeration and subsequently re-dispersed in distilled water as necessary. The bioreduction of selenium ions by *Exserohilum rostratum*, along with the maximum absorbance of the synthesized selenium nanoparticles (SeNPs), was assessed utilizing an ultraviolet–visible spectrophotometer (Dual Beam UV-1800). Spectra were analysed within the region of 200-600 nm for identifying surface plasmon resonance in biosynthesized Se-NPs. FT-IR analysis was conducted over the spectral range of 400–4000 cm^{-1} to recognize the biomolecules that participate in the reduction and stabilization of Se-NPs. The topography was examined through field-emission scanning electron microscopy (FESEM) as well as energy-dispersive X-ray spectroscopy EDX (JSM 6360 LV). An accelerating voltage between 10 and 15 kilovolts was employed to explore the topographic structure of the sample. The size distribution of selenium NP was conducted using ImageJ software. The resultant Se-NPs were examined through X-ray diffraction (XRD) patterns (Philips). The equipment utilized Ni-filtered radiation composed of Cu-K with a wavelength of 1.5405 Å and a proportional counter. It functioned at 40 kV and 30 mA. The Se-NPs' crystallographic nature was examined for 2 hours at temperatures ranging from 10 to 80°C. The PANalytical X'pert HighScore Plus version 4.0 software analysed XRD data via Scherrer's equation to determine the average crystalline size of the synthesized selenium nanoparticles.

Antioxidant Activity

One of the key objectives of the research is to examine the antioxidant activity of SeNPs synthesized from *Exserohilum rostratum*. For this purpose, SeNPs were used over a wide range of concentrations (62.5, 125, 250, 500, and 1000µg/mL) for evaluating the radical scavenging ability (RSA) against 2,2-diphenyl-1-picrylhydrazyl (DPPH) free radicals. A stock solution was prepared by adding one mM DPPH radical solution in 95% ethanol. During the experimental procedure, 800 µL of a solution of DPPH was added with 200 µL of each concentration of biosynthesized Se-NPs. The mixture was afterward incubated in the dark at a stable temperature of 25 ◦C for 30 minutes, followed by centrifugation for 5 minutes at 13,000 rpm. Each of the concentrations was measured at 517 nm against a blank, adopting ascorbic acid as the standard marker. Percentages of free radical scavenging were determined using Eq. 1 [38].

$$\text{DPPH scavenging activity } (\%) = \frac{A_C - A_T}{A_C} \times 100$$

Where, A_C = Absorbance of ascorbic acid (control). A_T = Absorbance of selenium nanoparticles.

All tests were done in triplicate, and the outcomes are shown as mean ± SD.

Cytotoxicity Assay, Anti-Tumor and Synergistic Evaluation of Selenium Nanoparticles (SeNPs) with Chemotherapeutic Agent

Cell culture

Healthy human breast epithelial cells (HBL-100) and cancer cells from human breast cancer (MCF-7) and prostate adenocarcinoma (PC3) were obtained from the tissue culture laboratory at the Department of Biology, College of Education for Pure Science, University of Basrah, Iraq. Cells were cultivated in RPMI-1640 enriched with fetal bovine serum 10%, penicillin 100 units/

ml, and streptomycin 100 µg/ml upon achieving confluence to form a monolayer. In summary, following a single wash of the cell culture with 2 ml of PBS solution, the cells were removed from the flask utilizing an equivalent volume solution of trypsin-utilizing, suspended cells were cultured in RPMI 1640 media enriched with 10% (v/v) fetal bovine serum (FBS), 100 U/mL penicillin, and 100 µg/mL streptomycin, and were inoculated into a 25-cm flask at 37° C. The suspension cells were bisected for proliferation. The proliferating cells were subsequently transferred to new flasks containing RPMI-1640 (5 ml) with 10% fetal bovine serum, incubated for 24 hours at 37°C, 5% CO_2. Upon reaching 80% confluence, this procedure was conducted on a biweekly basis. [39].

Cytotoxicity Assessment of (SeNPs) and Combination Effect

An initial cytotoxicity assay was performed to evaluate the biosafety of SeNPs synthesized from *Exserohilum rostratum* on a regular cell line (HBL-100), applying the MTT assay (Bio World, USA). Cells were plated in 96-well plates at a density of 1×10^4 cells per well and incubated overnight at 37°C to facilitate monolayer formation. SeNPs were injected at concentrations of 62.5, 125, 250, 500, and 1000 µg/ml, with each concentration tested in triplicate. Controls consisted of untreated wells, wells treated with 0.1% DMSO (solvent control), and serum-free wells (negative control). Following a 72-hour exposure period, 100 µL of MTT reagent was added to each well. The half-maximal inhibitory concentration (IC_{50}) of SeNPs on normal cells was calculated and applied as a benchmark to determine safe dosages in subsequent tests. Absorbance was quantified at 620 nm utilizing a microplate reader. SeNPs were subsequently tested on human cancer cell lines (MCF-7 and PC-3), via cell viability quantified using the MTT assay. Only concentrations determined to be non-toxic or minimally toxic to normal cells were tested on the cancer cell lines. The aim was to assess the selective cytotoxic effects of SeNPs on malignant cells, ensuring the preservation of normal cell viability. Cell viability inhibition was estimated using the following formula [40].

$$\text{Inhibition rate } (\%) = \frac{OD_C - OD_S}{OD_C} \times 100$$

Where; ODC = mean optical density of untreated wells; ODS = optical density of treated wells.

The inhibitory concentration (IC50) is the concentration that kills 50% of cells.

The synergistic effect

The potential synergistic effect was evaluated through the use of the MTT assay. The IC50 value was used as a measure to determine dosing factors in the current study. Based on IC_{50} values, a combination of Se NPs and the chemotherapeutic agent (doxorubicin) was administered to cancer cell lines. The cells were treated with varying concentrations of both agents, individually and in combination, under standardized culture conditions. The combination of the interaction (synergistic, additive, or antagonistic) between Se-NPs and doxorubicin was quantitatively analyzed using the Chou–Talalay method via CompuSyn software (version 1). The combination index (CI) was calculated based on dose-effect relationships obtained from cell viability assays. The combination index (CI) was interpreted as follows: CI < 0.9 = synergistic effect, CI 0.9–1.1 = additive effect, CI > 1.1 = antagonistic [41].

Statistical Analysis

The statistical studies of the antioxidant activity, cytotoxicity, and anticancer activity of endofungal-SeNPs occurred using the analysis of variance (ANOVA) test, with means ± standard deviation (SD) utilizing SPSS version 16. The evaluation focused on the differences in antioxidant responses between selenium nanoparticles and the standard control (ascorbic acid) across various concentrations. A nonlinear regression approach utilizing a sigmoidal dose-response curve was employed to determine IC_{50} values, which represent the concentration necessary to inhibit 50% of DPPH radicals. This statistical method facilitated the precise assessment of the antioxidant efficacy and anticancer activity of EX-SeNPs. We assessed the synergistic effects of selenium nanoparticles (EX-SeNPs) in combination with doxorubicin (Doxo) on cancer cell lines utilizing the CompuSyn software program algorithm, which is fitted to the Chou-Talalay lines harmonic index (CI) method, which is derived from the law of mass action. CI<1 indicates synergistic interaction, whereas CI >1 is antagonistic, and CI=1 is considered additive.

RESULTS AND DISCUSSION

Mycoendophyte culture, extracellular Mycosynthesis of Selenium nanoparticles

Exserohilum rostratum Basra_A15 was isolated from the stems of *Schoenoplectiella articulata* (family Cyperaceae) obtained from natural environments in Basra, Southern Iraq, in October 2024. On PDA plates, the morphological traits of *E. rostratum* were observed to be in the form of a circle, with a rich brown upper surface and a black lower surface, characterized by prominent growth of aerial mycelium with a woolly or cotton-like texture. A fungal endophyte's ITS ribosomal DNA (rDNA) was sequenced and

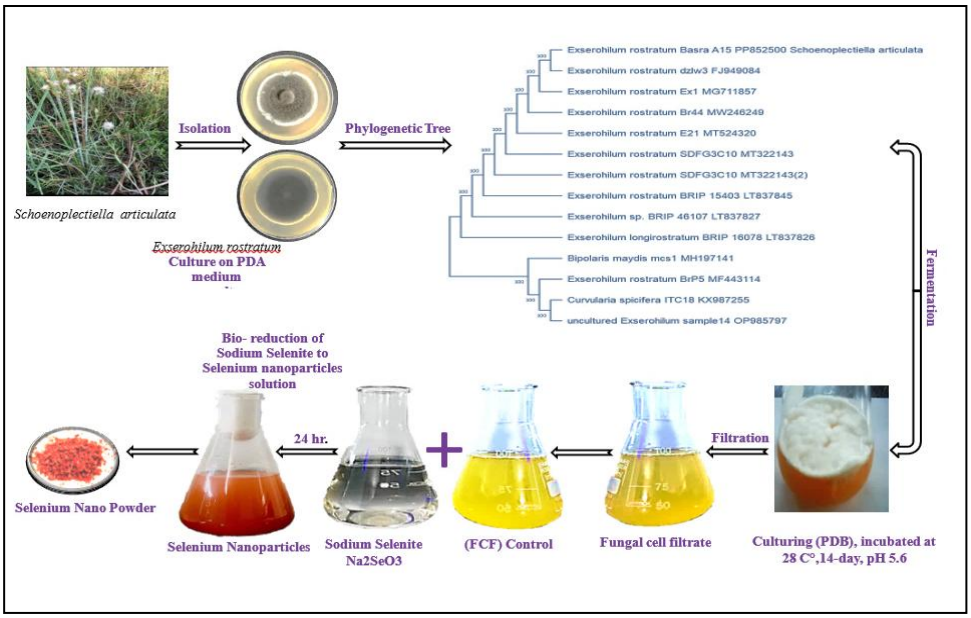

Fig. 1. Endophytic fungus *Exserohilum rostratum*; isolation, identification, fabrication, and purification of Nano Selenium.

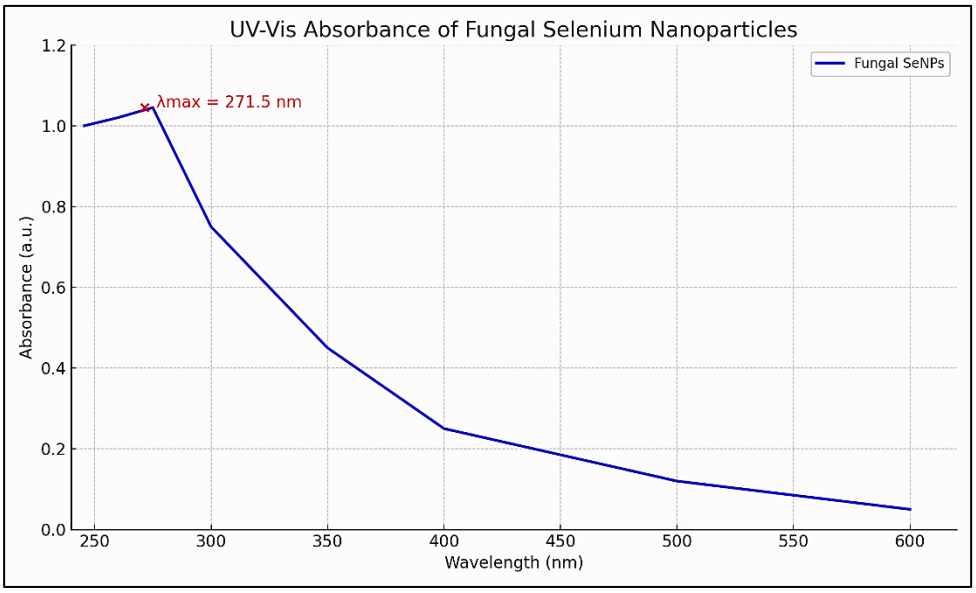

Fig. 2. Ultraviolet-visible spectrum of Endo-Myco-synthesized SeNPs.

compared against existing genetically close strains in GenBank. The comparison studies revealed complete congruence and coverage with multiple E. rostratum strains and the reference dzlw3 (GenBank No.: FJ949084.1). A strain sequence was officially submitted to the GenBank database under accession number PP852500. Free cell filtrate (FCF) extracted from fungal cultures in PDB fermentation medium, maintained for two weeks, and treated via Na2SeO3 solution, showed a turn in colour from light-yellow to ruby-red, implying production of selenium nanoparticles. Fig. 1.

Detecting and Characterizing Myco-Synthesized SeNPs

Ultraviolet-visible Spectroscopic

UV-visible spectroscopy was initially employed to monitor the successful synthesis of Se-NPs, which documented their creation in mycelium-free filtrate supplemented with a one mM sodium selenite solution. The absorbance spectra of the SeNPs, as seen in Fig. 2, display a pronounced and extensive peak at 271.50 nm with an absorption of approximately 1.045, within the range of 200–600 nm.

The maximum absorption at 271.5 nm is attributed to Se^0, caused by the free electron coherent oscillation over exterior selenium particles, a phenomenon recognized as Surface Plasmon Resonance absorption. The peak observed is characteristic of the surface plasmon resonance (SPR) of selenium nanoparticles. It aligns with previously reported values in the literature, typically from green synthesis routes using fungi, where biomolecules such as proteins, flavonoids, and phenolic compounds contribute to reducing sodium selenite to elemental (Se^o). Previously reported investigations revealed that the SeNPs exhibit multiple absorption bands in the UV-visible region, which is attributed to the synthesizing method, influenced by fungal metabolites that serve as reducing and capping agents. [15,42]. Interestingly enough, SeNPs were seen to show a broad absorption peak at 270 nm [43]. These results verify the efficiency of the fungus used in the current study to act as a bio-catalyst in the reduction of SeO_3^2 to Seo. On the other hand, SeNPs from *Acinetobacter sp*. SW30 was also seen to show two maxima of absorbance at 300 nm and 500 nm [44]. SeNPs synthesized by radiation from gamma with *Monascus purpureus* had the strongest SPR peak at 593 nm [22]. Islam et al. [45], in their study, used *Fusarium oxysporum* as a bio-catalyst and observed a prominent peak of absorption at 265 nm, indicative of the formation of SeNPs in reasonable quantity and shape. Spectral studies of green SeNPs synthesized in the presence of the fungus *Nigrospora gullinensis* showed a peak of absorption at 265 nm [46]. *Penicillium expansum* ATCC 36200 was employed to synthesize SeNPs with a peak at around 295 nm. [27]. Kumar et al. [47] reported the utilization of crude cell-free protein from *Geobacillus sp.* to biosynthesize SeNPs that showed SPR absorption at 349 nm. Divergent results may be attributed to differences in particle size.

FT-IR Spectroscopy

The O-H and N-H functional groups in amino acids as well as proteins account for an intense peak at 3298.28, which shifts to 3431.36 cm^{-1} upon Se-NPs incorporation. These peaks at 1656.85 and 1535.34 cm^{-1} show evidence of C-N stretching vibrations characteristic of aromatic amines. These additional peaks in Se-NPs' FT-IR spectrum can be ascribed to interactions between

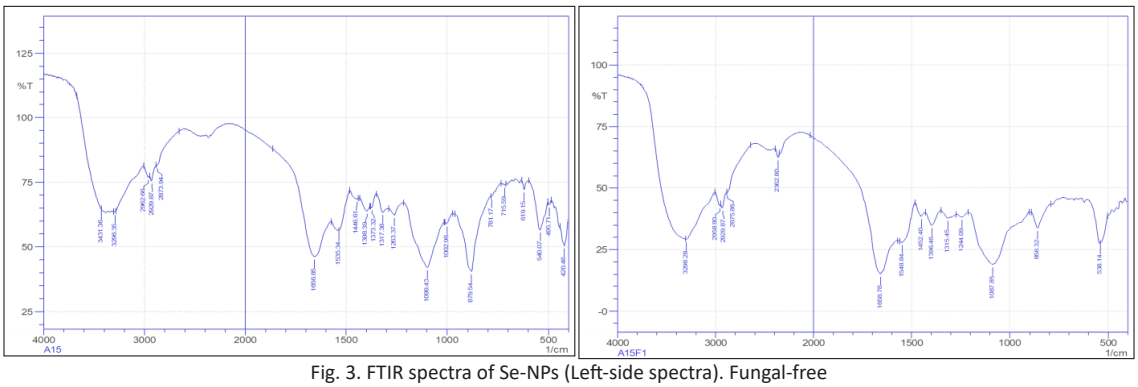

Fig. 3. FTIR spectra of Se-NPs (Left-side spectra). Fungal-free

the metabolites in fungus-free filtrate biomass and sodium selenite during reduction, and also to capping of synthesized selenium nanoparticles. A moderate peak of 2962.66 cm^{-1} reflects C-H stretching of the presence of alkanes, and the medium peaks in the region of 1656.85-1099.43 cm^{-1} in carboxylic acids can be attributed most likely to O-H stretching. Calcinated selenium nanoparticles had a peak at 540.07 cm^{-1}, Saied et al. [29] showing the presence of proteins that bind with selenium nanoparticles and may be involved in stabilizing them. It should be remembered that protein dimensions and structures are significant parameters [28, 48]. Thus, cysteine residues and free amine groups in proteins enhance protein-nanoparticle interaction (Fig. 3) [49].

X-ray diffractometer evaluation

Investigating XRD, shown in Fig. 4, provided additional insight into the structural characteristics of biosynthesized Se-NPs from Exserohilum rostratum, which exhibited five distinct peaks at (100), (101), (111), (102), and (003). These peaks correspond with the Bragg diffraction of 2θ values at 23.3430°, 29.7252°, 41.3430°, 43.7707°, and 55.3930°, respectively. The resultant XRD pattern of SeNPs synthesized from *Exserohilum rostratum* was juxtaposed with the crystallographic structure of SeNPs as per JCPDS reference card No. 00-042-1425. Based on the XRD analysis, this technique demonstrates significant potential for characterizing both bulk and nanomaterials, effectively analyzing crystallized materials by displaying configuration phases, preferred crystal orientations, size, crystallization, separation, and defects within the crystals. Furthermore, the average crystalline size was calculated to be 51.15 nm, applying the Debye-Scherrer formula, which depended on the full width at half maximum (FWHM) of the most prominent peak of the manufactured nanoparticles [28].

A recent study determined that the endophytic fungi *Fusarium equiseti*, *Aspergillus quadrilineatus*, *A. ochraceus*, and *A. terreus* produced crystallites with sizes of 30.1, 55.4, 45.2, and 30.9 nm, respectively, as measured by XRD analysis [28]. In a separate study, El-Sayyad et al. [30] synthesized Se-NPs from the fungus *Penicillium chrysogenum* and calculated that the mean size of the particles was approximately 33.84 nm using Debye-Scherrer's equation.

AFM Analysis

AFM surface morphology of fungus-synthesized SeNPs showed relatively rough surface morphology with maximum peaks of height up to 34.28 nm in nanosized. The 3D surface mode revealed an irregular yet biologically representative surface with hemispherical and spherical particles, characterized by natural

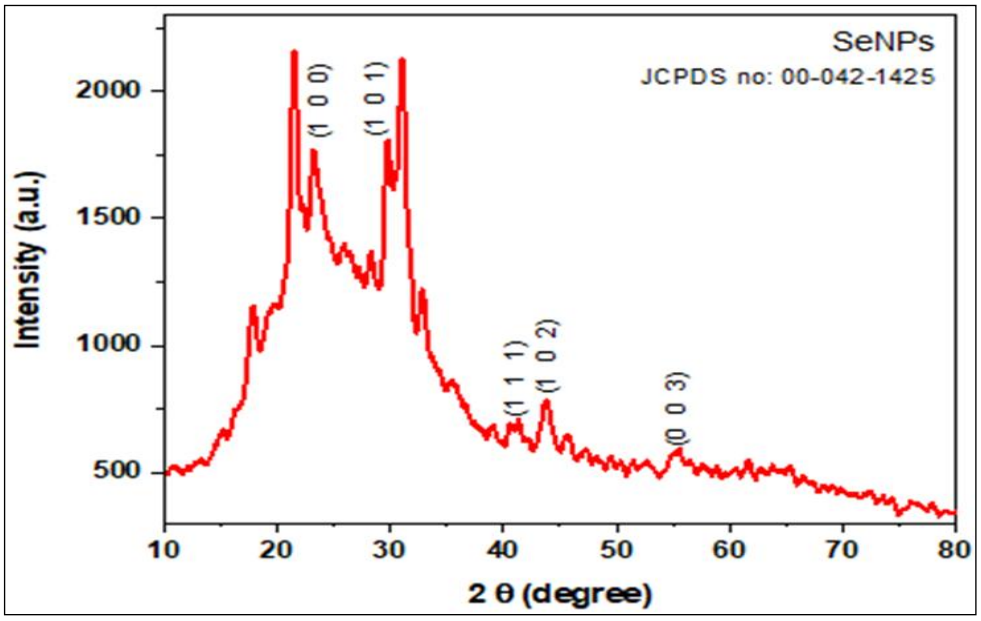

Fig. 4. XRD of SeNPs.

nucleation and stabilization in the presence of fungus metabolites. The results are shown. The threshold detection revealed 517 particles on the scanned surface, achieving 15.14% coverage and a density of 2.1 × 10^7 particles per mm^2. The uniform packing and morphology resulting from the efficient biosynthetic process may be governed by the fungus's enzymes and reducing agents, which promote uniform particle growth. The size distribution of particles uncovered a mean diameter of 63.92 nm, with a large majority of particles of a size in the range of small size (10–100 nm) type observed in histogram Fig. 5. There were few large particles also observed, represented in it which reflect the natural size range of green synthesis methods carried out. The relatively low value of Z-max height and a uniform range of sizes reflect a stable and reproducible biosynthetic environment. Such a surface structure, characterized by high surface area, moderate roughness, and a uniform size range, is proper in biomedical applications due to its increased bioavailability and reactivity in prospective antioxidant, antibacterial, or therapeutic systems.

FESEM/EDX

The FESEM reveals the morphology and particle dimensions of the Se-NPs, which are found to be nearly sphere-like in form with a smooth outer surface. FESEM analyzed the powders of biosynthesized samples. During the process, the operating voltage was maintained at 10 kV with a vacuum pressure of 5–10 Torr, as measured on a scale of 100k× magnification. The FESEM analysis indicated that biosynthesized SeNPs are homogenous and monodispersed Fig. 6, a. Moreover, the morphological analysis revealed that biosynthesized Se-NPs mostly exhibit a spherical shape (Fig. 6 b). The size of particles biosynthesized Se-NPs varied from 8.17 to 19.61 nm with a mean diameter of 14.26 nm.

Earlier, it was reported that the NPs, prepared using the aqueous extract of *Clausena dentata* leaves, exhibited a spherical form, often measuring 46–78 nm in diameter [50].

Moreover, the EDX analysis spectrum exhibited a strong and sharp peak of elemental selenium, as seen in Fig. 6c; the total percentage was 87.98%. The prior study conducted on the leaf extract of *Withania somnifera* indicated that the narrow width of the EDX profile demonstrates that the element selenium is highly purified [51].

Antioxidant Activity

The free radical-scavenging capability of selenium nanoparticles was evaluated using the DPPH test, compared to ascorbic acid as a control. Table 1 shows that SeNPs are very effective at reducing free radicals, achieving the highest reduction of 83.3 ± 1.74% at a concentration of 1000 µg/ml. Although this activity was consistently

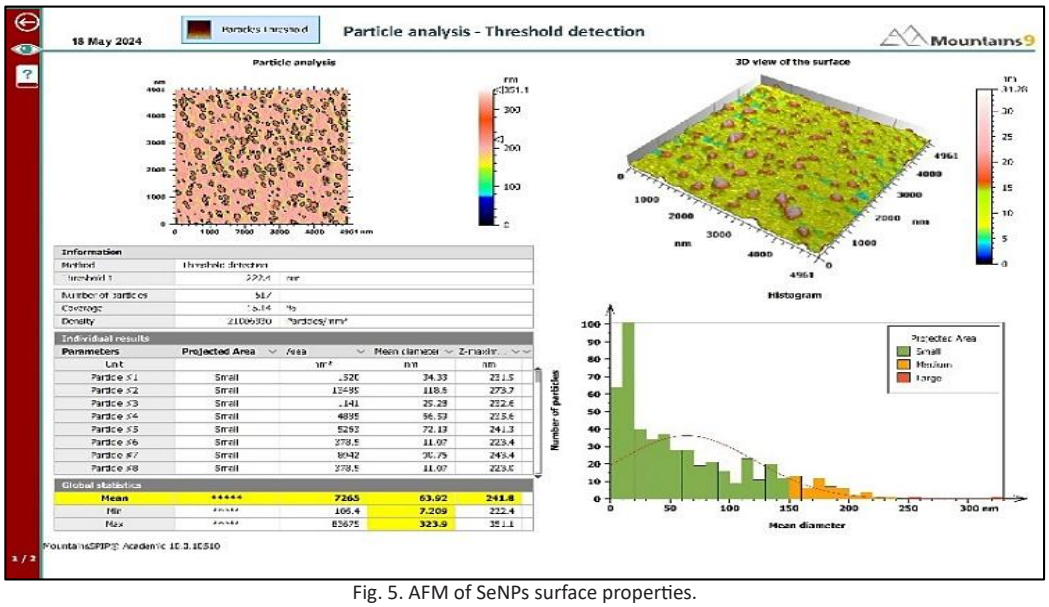

Fig. 5. AFM of SeNPs surface properties.

lower than that of the standard antioxidant, ascorbic acid (which showed 91.53 ± 4.31% at the same concentration), the SeNPs still exhibited notable antioxidant potential. The effectiveness of SeNPs declined at lower concentrations, with RSA dropping to 23.93 ± 4.74% at 62.5 µg/ml, suggesting that higher concentrations are required for significant activity. The calculated IC_{50} value for SeNPs (158.3 µg/ml) was considerably higher than that of ascorbic acid (60.96 µg/ml), indicating that although SeNPs are less potent than the control, they still possess moderate antioxidant capacity. This activity is attributed to the distinctive redox characteristics of selenium in the nanostructures combined with biologic capping agents provided by *E. rostratum*, which may contribute to electron

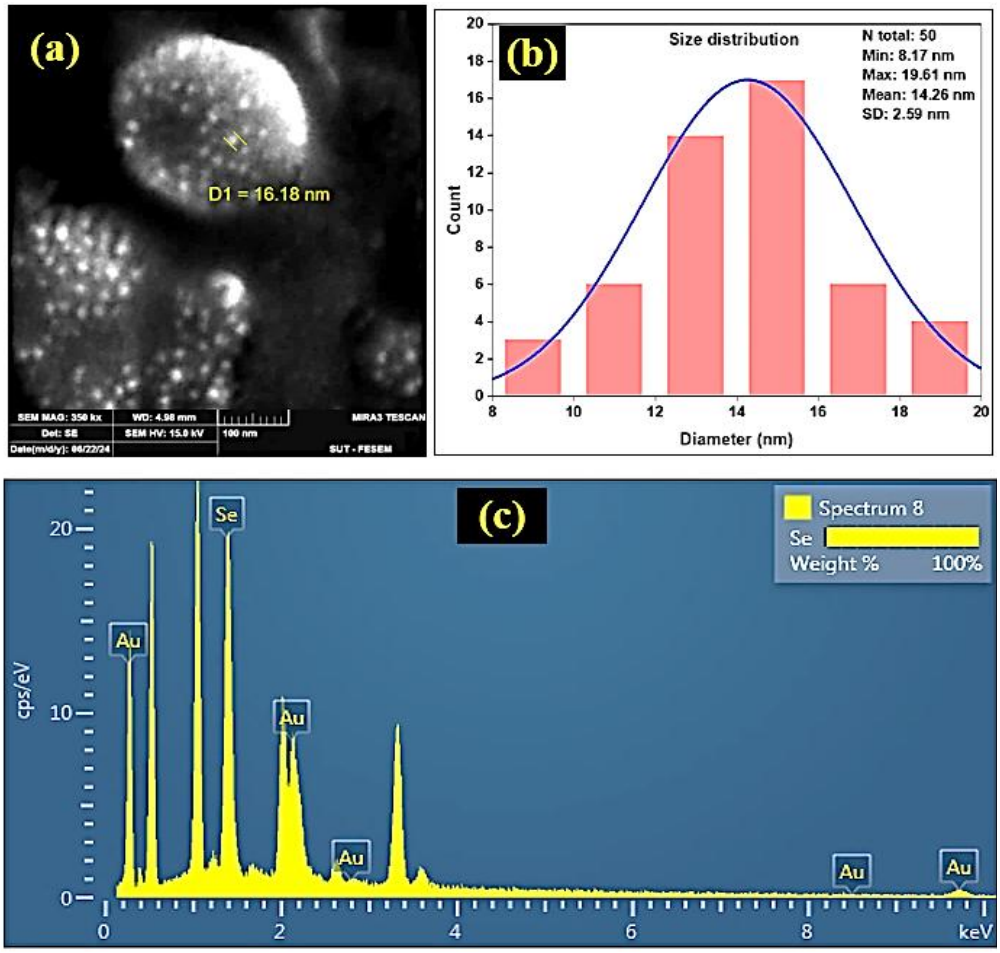

Fig. 6. (a) FESEM image. (b) The histogram of particle size distribution from the (a) image. (c) EDX- analysis of myco-synthesized SeNPs.

Table 1. DPPH activity of SeNPs synthesized by *Exserohilum rostratum.*

Concentration. (µg ml^{-1})	RSA (%)	
	Control (Ascorbic Acid)	*Ex*-SeNPs
1000	91.53 ± 4.31	83.3 ± 1.74
500	80.72 ± 6.81	66.09 ± 1.33
250	77.64 ± 1.25	55.3 ± 1.76
125	66.15 ± 1.08	46.24 ± 3.41
62.5	46.31 ± 0.42	23.93 ± 4.74
IC_{50} (µg ml^{-1})	60.96	158.3

donation capabilities, thereby neutralizing free radicals [14].

In a similar study, SeNPs synthesized from endophytic fungi demonstrated DPPH-scavenging efficiencies of 93.8±9.5% for *Aspergillus quadrilineatus*, 83.6±6.3% for *A. ochraceus,* 79.2±9.3% for *A. terreus,* and 79.8±4.7% for *Fusarium equiseti*, compared to the 100% activity of scavenging observed in ascorbic acid [28]. The antioxidant potential of SeNPs produced by the endophytic fungus in the present study is motivating and promising, particularly at the applied concentration, suggesting a new avenue for exploring nano-selenium as an antioxidant source. The Se-NPs' antioxidant effects can be attributed to their capacity to enhance selenoenzymes, including peroxidase, which safeguards cells from the detrimental impacts of the radicals in vivo environments. Antioxidants in NPs may result from the neutralization and inhibition of free radical formation through electron transfer [52]. Nanoparticles' unique properties, in particular, high surface area relative to their size, can enhance the antioxidant effect. The following Fig. 7 represents the antioxidant activity of biosynthesized Endofungal Se nanoparticles (*EX*-SeNPs).

Cytotoxicity Assay and Synergistic Evaluation of Selenium Nanoparticles (SeNPs) with Chemotherapeutic Agents

Cytotoxicity Assessment of Selenium Nanoparticles (SeNPs)

The cytotoxicity screening of Se-NPs on regular cell lines is a crucial preliminary step towards the assessment of their biosafety profile, which is paramount to their potential biomedical and therapeutic uses. Cytotoxicity testing of selenium nanoparticles (SeNPs) on the HBL-100 cell line (human breast epithelium) revealed negligible effects at lower concentrations. The cytotoxicity of SeNPs produced by *Exserohilum rostratum* reveals a promising selective toxicity profile, with significantly greater efficacy against cancer cells compared to normal cells. The cytotoxicity of SeNPs produced by *Exserohilum rostratum* reveals a promising selective toxicity profile, with substantially greater efficacy against cancer cells compared to normal cells. The IC50 value in normal HLB100 cells is very high at 405.9 µg/mL, which suggests low toxicity and may point towards

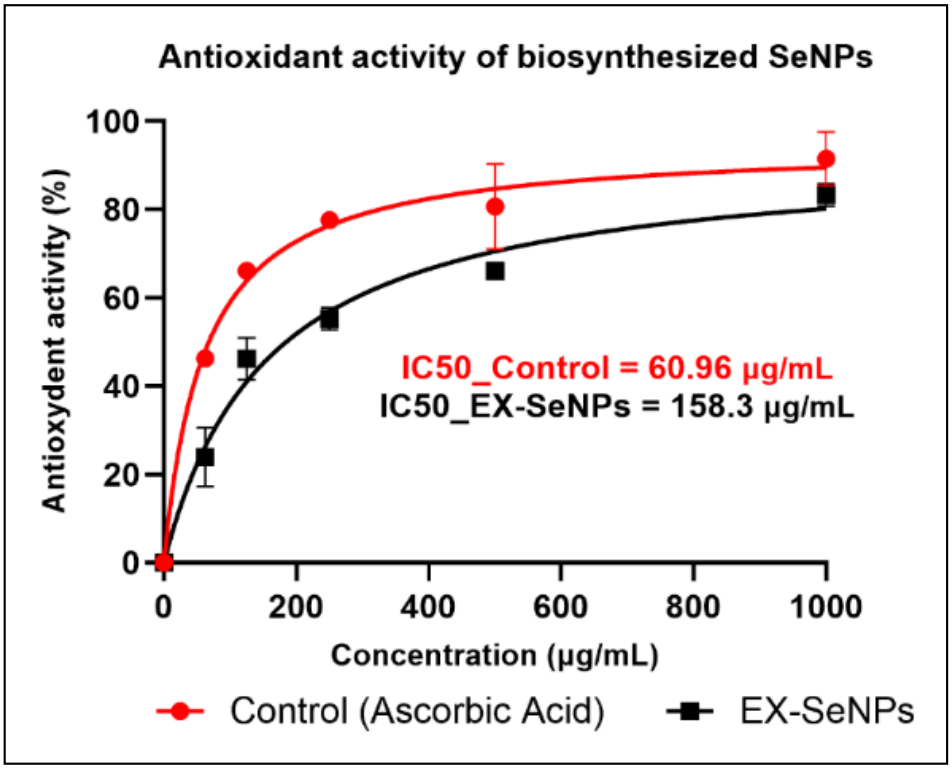

Fig. 7. Antioxidant effects of biosynthesized SeNPs.

biocompatibility with minimal toxic activity on healthy tissue. Conversely, the lower IC50 values of cancer cell lines 84.0 ± 2.06 µg/mL (PC3 prostate cancer) and 134.67 ± 1.98 µg/mL (MCF7 breast cancer) reveal potent anticancer activity with high sensitivity against the more sensitive PC3 cells. According to standard cytotoxicity classification criteria, compounds with IC_{50} values below 100 µg/ml are generally regarded as exhibiting "potent" anticancer activity [53]. Thus, the observed IC_{50} values confirm the potent and selective cytotoxic nature of fungal-derived SeNPs toward malignant cells, particularly the PC3 line. Thus, the observed IC_{50} values confirm the potent and selective cytotoxic nature of fungal-derived SeNPs toward malignant cells, particularly the PC3 line. The results correspond with earlier research related to the preferential activity of fungal-derived SeNPs, which is attributed to their greater biocompatibility and cancer-specific targeting [54, 55].

Cancer cells with higher levels of ROS and compromised antioxidant defenses are more vulnerable to SeNP-induced oxidative stress, which initiates apoptosis by inducing mitochondrial injury and DNA damage [53]. The higher sensitivity of PC3 compared to MCF7 can indicate differences in membrane permeability or efflux pump activity, as prostate cancer cells are known to exhibit greater endocytic uptake of nanoparticles [56,57].

Furthermore, the use of endophytic fungus *Exserohilum rostratum* in biosynthesis is expected to render greater stability and bioactivity, as fungal systems have been shown to yield nanoparticles with engineered surface chemistries that promote therapeutic efficacy. The following Fig. 8 indicates the inhibition rate of normal cells and cancer cell lines.

Enhancement of SeNPs Cytotoxicity via Doxorubicin

The findings indicate that the antitumor efficacy of myco-synthesized selenium nanoparticles is concentration-dependent, with preferential activity against cancerous cells (PC3 and MCF-7) and minimal toxicity to normal mammary epithelial cells (HBL-100). Specifically, SeNPs exhibited IC_{50} values of 84.0 ± 2.06 *µg/m*l for PC3 and 134.67 ± 1.98 *µg/m*l for MCF-7cell lines. Compared to the chemotherapeutic agent doxorubicin (Doxo), which demonstrated higher potency, with IC_{50} values of 20.22 *µg/ml* for PC3, 10.7 *µg/mL* for MCF-7. Nevertheless, the co-administration of Myco-SeNPs with the therapy Doxo significantly enhanced anticancer efficacy, indicating an increase in cytotoxicity, as evidenced by the reduced IC_{50} values of 22.17 *µg/m*l for PC3 and 50.55 *µg/m*l for MCF-7. These findings support the hypothesis of a synergistic interaction, therefore minimizing the toxicity and dosage of the drug to improve its effectiveness.

Consequently, the observed improvement may be attributed to enhanced cellular uptake, improved bioavailability, and SeNPs-induced modulation of apoptosis-related signaling pathways, as suggested in prior studies [58, 59]. Therefore, fungal-derived SeNPs represent

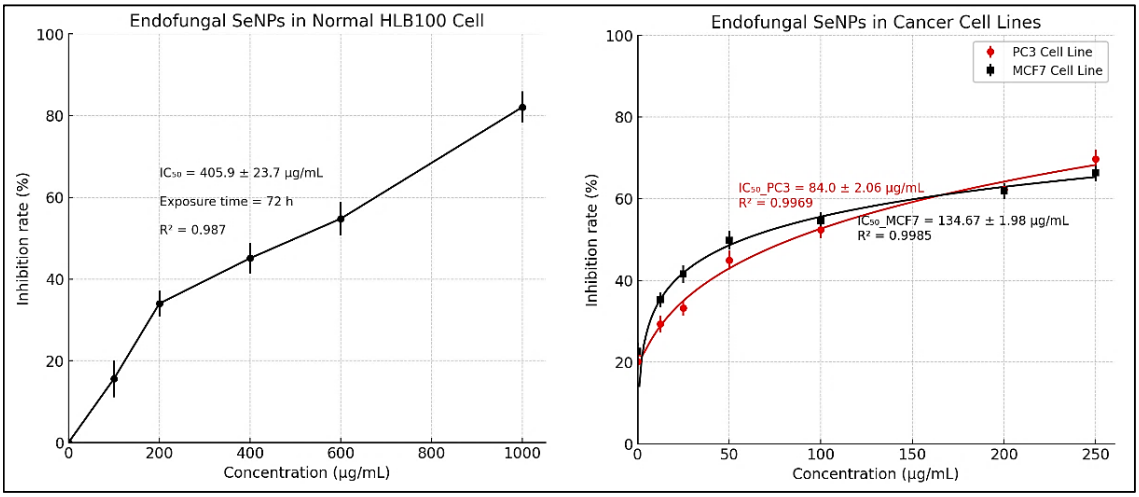

Fig. 8. Inhibition rate (%) of normal cells (Left-side image) and cancer cell lines (Right-side image).

a promising adjuvant strategy in cancer chemotherapy. Fig. 9 shows the dose-dependent inhibition rates of MCF7 and PC3 cell lines treated with fungal-SeNPs, Doxo, and their combination.

Synergistic Effect and Biocompatibility

To evaluate the synergistic interaction between biosynthesized selenium nanoparticles (EX-SeNPs) and the chemotherapeutic drug doxorubicin (Doxo), the combination index (CI) was calculated using the Chou-Talalay method. The CI values plotted against the fraction affected (Fa) for both PC3 and MCF7 cell lines provide insights into the nature of the drug interaction SeNPs. Following Tables 2 and 3 present the combination index (CI) data of the combination of selenium nanoparticles (EX-SeNPs) and doxorubicin (DOXO) for PC3 and MCF cell lines. The combination Index (CI), which indicates the extent of synergy through a decline in values and an increase in the Fa. In the PC3 cell line, specifically, the values of CI decline drastically from 246.96 at Fa = 0.05 (indicative of strong

Table 2. CI and Fa Data for PC3 Cell Line (EX-SeNPs + Doxorubicin).

Fa	CI ± SD	Interpretation
0.05	10.74 ± 1.22	Antagonism
0.1	2.781 ± 0.235	Antagonism
0.15	1.206 ± 0.0802	Additive
0.2	0.643 ± 0.034	Synergy
0.25	0.382 ± 0.0162	Strong synergy
0.3	0.243 ± 0.008	Powerful synergy
0.35	0.161 ± 0.004	Powerful synergy
0.4	0.11 ± 0.002	Powerful synergy
0.45	0.0757 ± 0.0008	Hyper synergy
0.5	0.0527 ± 0.0003	Hyper synergy
0.55	0.0367 ± 0.0003	Hyper synergy
0.6	0.0254 ± 0.0004	Hyper synergy
0.65	0.0173 ± 0.0004	Hyper synergy
0.7	0.0115 ± 0.0003	Hyper synergy
0.75	0.0073 ± 0.0003	Hyper synergy
0.8	0.0043 ± 0.0002	Hyper synergy
0.85	0.0023 ± 0.0001	Hyper synergy
0.9	0.001 ± 0.0001	Hyper synergy

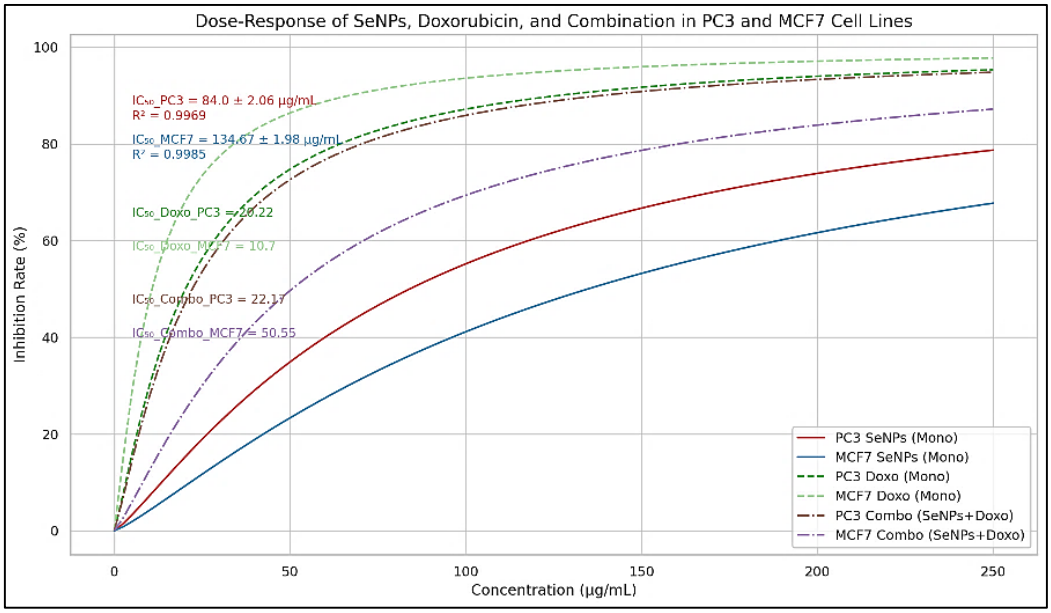

Fig. 9. Dose-dependent inhibition rates of MCF7 and PC3 cell lines treated with fungal-SeNPs, Doxo, and their combination.

antagonism) to 0.00016 at Fa = 0.90 (reflecting extreme synergy). A similar trend is observed for the MCF7 cell line, where the values of CI decline from 10.74 to 0.00101 across the same range of Fa. The Chou-Talalay hypothesis posits that values of CI below 1 indicate synergy, those below 0.3 signify strong synergy, and those below 0.1 denote very strong or hyper-additive synergism [41]. The results unequivocally prove that as the cytotoxicity of the compound increases, the interaction between EX-SeNPs and Doxo becomes more cooperative, which may further increase therapeutic efficacy at lower dosages. The enhanced synergy noted at high values of Fa indicates that small administrations of the two drugs can achieve cancer cell inhibition, and the approach is an optimal strategy in the chemotherapy regimen to reduce side effects [60].

One of the key factors contributing to the observed synergy is the experimental repeatability and precision of the data, demonstrated by the low standard deviation values for the CI values. For instance, in PC3 cells with Fa of 0.50, the CI is measured as 0.03433 ± 0.00013, and in the case of MCF7, the values are 0.05273 ± 0.00028, indicative of very high experimental consistency. The high reproducibility is critical to the potency of EX-SeNPs as synergistic compounds in combination therapies. Mechanistically, from the perspective of the mechanism, the EX-SeNPs are known to influence many cell pathway activities involving the production of reactive oxygen species, the triggering of malfunctioning mitochondria, and modulating apoptosis-related proteins, such as Bcl-2 and caspases [61,62]. With doxorubicin (Doxo), which is an intercalation inhibitor of topoisomerase II, when administered along with the EX-SeNPs, the latter are expected to reduce the cancer cell resistance to the stress imparted by the former, leading to enhanced cell death. Further, the biosynthesis of EX-SeNPs using biomaterials leads to the introduction of biologically active capping molecules (like proteins, phenolics, and polysaccharides) on the EX-SeNPs, which stabilize the particles as well as may induce supplementary antitumor action [63,64].

From the perspective of biocompatibility, biosynthesized selenium nanoparticles (EX-SeNPs) are superior to chemically synthesized particles. Selenium, a crucial essential element in human physiology, is engaged in the regulation of anti-oxidant defenses through the action of selenoenzymes, including glutathione peroxidase and thioredoxin reductase [15,42]. Nano selenium, on the contrary, exhibits higher safety profiles, particularly when fabricated through eco-friendly biological routes. Fungal endophytes such as *Exserohilum rostratum* are ideal biogenic producers of nanoparticles since the former produces extracellular metabolites that not only enhance ion reduction and offer biocompatible capping but also reduce immunogenic responses and systemic toxicities inherent in nanomaterials produced through chemical routes [43,65].

From the perspective of biocompatibility, biosynthesized selenium nanoparticles (*EX*-SeNPs) are superior to chemically synthesized

Table 3. CI and Fa Data for MCF7 Cell Line (EX-SeNPs + Doxorubicin).

Fa	CI ± SD	Interpretation
0.05	246.96 ± 67.47	Antagonism
0.1	24.2 ± 4.9	Antagonism
0.15	5.82 ± 0.914	Antagonism
0.2	2.01 ± 0.247	Antagonism
0.25	0.84 ± 0.0796	Synergy
0.3	0.4 ± 0.028	Strong synergy
0.35	0.2 ± 0.01	Powerful synergy
0.4	0.11 ± 0.0033	Powerful synergy
0.45	0.06 ± 0.0009	Powerful synergy
0.5	0.03 ± 0.0001	Hyper synergy
0.55	0.02 ± 0.0003	Hyper synergy
0.6	0.01 ± 0.0002	Hyper synergy
0.65	0.01 ± 0.0001	Hyper synergy
0.7	0.0036 ± 0.0001	Hyper synergy
0.75	0.00193 ± 0.0001	Hyper synergy
0.8	0.00097 ± 0.00002	Hyper synergy
0.85	0.00043 ± 0.00001	Hyper synergy
0.9	0.00016 ± 0.00001	Hyper synergy

particles. Selenium, a crucial essential element in human physiology, is engaged in the regulation of antioxidant defences through the action of selenoenzymes, including glutathione peroxidase and thioredoxin reductase. [15,42]. Bulk selenium compounds, on the other hand, exhibit narrow therapeutic windows and an inherent potential for toxicities. Nano selenium, on the contrary, exhibits higher safety profiles, particularly when fabricated through eco-friendly biological routes. Fungal endophytes such as *Exserohilum rostratum* are ideal biogenic producers of nanoparticles since the former produces extracellular metabolites that not only enhance ion reduction and offer biocompatible capping but also reduce immunogenic responses and systemic toxicities inherent in nanomaterials produced through chemical routes [43,66].

Moreover, synergy with Doxorubicin implies that decreased dosages of each of the drugs may prove to be therapeutically effective, thereby lessening the overall burden on healthy cell populations and reducing many side effects inherent in the use of Doxorubicin. In the context of the approach, EX-SeNPs act not just as mere enhancers of drugs but also as protective molecules that modulate cancer chemotherapy towards targeted, efficient, and safer ends. The use of these biosynthesized nanomaterials in combination chemotherapy protocols has the potential to revolutionize oncological treatment paradigms through cost-effective, environmentally sustainable, and patient safety-based alternatives [67-69].

Beyond the scope of the present findings, the biomedical versatility of nanoparticles continues to inspire novel therapeutic strategies. Their physicochemical tunability has been harnessed in gene therapy to achieve targeted delivery and controlled release systems, unlocking new possibilities for precision medicine [70]. The convergence of nanotechnology and artificial intelligence is accelerating this progress, enabling predictive modeling, structural optimization, and performance enhancement with unprecedented efficiency [71]. Antibacterial efficacy, as demonstrated in our study, resonates with similar outcomes observed in biogenic systems such as chitosan nanoparticles biosynthesized by Streptococcus thermophilus, where particle size, surface charge, and capping biomolecules dictated bactericidal potency [72]. In oncology, selenium nanoparticles have been shown to modulate critical signal transduction pathways in colorectal cancer models, underscoring their selective anticancer potential [73], while plant-derived variants with unique morphologies have advanced the frontier of tailored medical treatments [74]. Parallel to these approaches, mycofabricated silver nanoparticles synthesized by the endophytic fungus Papulaspora pallidula have exhibited remarkable dual functionality—combining potent anticancer and antibacterial activities [75], and further work has confirmed their broad-spectrum antimicrobial capacity against multiple human pathogens through eco-friendly synthesis routes [76]. Collectively, these advances reflect a global shift toward green nanotechnology, where sustainability and biomedical efficacy converge to redefine therapeutic innovation.

CONCLUSION

The current study successfully demonstrated the biosynthesis and biosafety of selenium at the nanoscale, mediated by the fungal endophyte *Exserohilum rostratum*. Comprehensive physicochemical characterizations confirmed the formation of stable, functional, and crystalline SeNPs. UV-Vis spectrum revealed a characteristic resonance surface plasmon peak at 271.5 nm, indicating the synthesis of spherical nanoparticles. FTIR analysis confirmed the role of fungal biomolecules throughout the reduction, stabilization, and capping processes. XRD, AFM, and FESEM-EDX collectively confirmed the crystalline structure, nanoscale size, and purity of the SeNPs. Biologically, the SeNPs exhibited moderate antioxidant activity (IC_{50} = 158.3 µg/ml) and selective cytotoxicity: higher IC_{50} values in normal HBL-100 cells (405.9 ± 23.7 µg/ml), and significantly lower IC_{50} values in cancerous cell lines (MCF-7 = 134.67 ± 1.98 µg/ml; PC3 = 84.0 ± 2.06 µg/ml), confirming their selective anticancer potential. Notably, combination treatments with doxorubicin significantly reduced the IC_{50} values (MCF-7 = 50.55 µg/ml; PC3 = 22.17 µg/ml), with combination indices (CI) reaching as low as 0.00016 for PC3, indicating a strong synergistic interaction. While our results affirm SeNPs' potential as safe and effective anticancer agents, the study was restricted to in vitro assays. Further research is essential to validate the pharmacokinetics, biodistribution, immune compatibility, and long-term toxicity in vivo. Moreover, the exact molecular mechanisms underlying the selective

cytotoxicity of SeNPs remain to be fully elucidated. Future studies should include transcriptomic and proteomic analyses, ROS generation assays, and apoptosis-related gene expression profiling. Expanding this research to include other endophytic fungal species may yield SeNPs with enhanced therapeutic properties. Incorporating SeNPs into advanced drug delivery platforms such as liposomes, polymeric carriers, or hydrogels could further improve target specificity and control drug release. From a translational perspective, scalable production processes ensuring reproducibility, purity, and functional integrity will be pivotal for clinical application. Furthermore, a systematic investigation into SeNPs' interaction with existing chemotherapeutics or immunotherapies can open new avenues for combination therapies in precision oncology.

ACKNOWLEDGEMENTS

The authors extend their appreciation to the authorities of the Microbiology Department at the College of Veterinary Medicine, University of Basra (Iraq), and the Central Research Laboratory for their invaluable support of this research, which forms a component of the first author's PhD program.

CONFLICT OF INTEREST

The authors declare that there is no conflict of interests regarding the publication of this manuscript.

REFERENCES

1. Sriharikrishnaa S, Suresh PS, Prasada K S. An Introduction to Fundamentals of Cancer Biology. Biological and Medical Physics, Biomedical Engineering: Springer International Publishing; 2023. p. 307-330.
2. Nikolaou M, Pavlopoulou A, Georgakilas AG, Kyrodimos E. The challenge of drug resistance in cancer treatment: a current overview. Clinical and Experimental Metastasis. 2018;35(4):309-318.
3. Daneshmand S, Ahmadi H. Androgen deprivation therapy for prostate cancer: long-term safety and patient outcomes. Patient Related Outcome Measures. 2014:63.
4. Reiss AB, Gulkarov S, Pinkhasov A, Sheehan KM, Srivastava A, De Leon J, et al. Androgen Deprivation Therapy for Prostate Cancer: Focus on Cognitive Function and Mood. Medicina. 2023;60(1):77.
5. Lumachi F, Brunello A, Maruzzo M, Basso U, Basso S. Treatment of Estrogen Receptor-Positive Breast Cancer. Curr Med Chem. 2013;20(5):596-604.
6. Nguyen PL, Alibhai SMH, Basaria S, D'Amico AV, Kantoff PW, Keating NL, et al. Adverse Effects of Androgen Deprivation Therapy and Strategies to Mitigate Them. Eur Urol. 2015;67(5):825-836.
7. Chen HHW, Kuo MT. Improving radiotherapy in cancer treatment: Promises and challenges. Oncotarget. 2017;8(37):62742-62758.
8. Kumar C, Pareri AU, Koijam AS. Breaking the Silence of Tumor Response: Future Prospects of Targeted Radionuclide Therapy. Anticancer Agents Med Chem. 2022;22(10):1845-1858.
9. LaVasseur C, Neukam S, Kartika T, Samuelson Bannow B, Shatzel J, DeLoughery TG. Hormonal therapies and venous thrombosis: Considerations for prevention and management. Research and Practice in Thrombosis and Haemostasis. 2022;6(6):e12763.
10. Malik S, Muhammad K, Waheed Y. Emerging Applications of Nanotechnology in Healthcare and Medicine. Molecules. 2023;28(18):6624.
11. Liu B, Zhou H, Tan L, Siu KTH, Guan X-Y. Exploring treatment options in cancer: tumor treatment strategies. Signal Transduction and Targeted Therapy. 2024;9(1).
12. Wang B, Hu S, Teng Y, Chen J, Wang H, Xu Y, et al. Current advance of nanotechnology in diagnosis and treatment for malignant tumors. Signal Transduction and Targeted Therapy. 2024;9(1).
13. Islam S, Ahmed MMS, Islam MA, Hossain N, Chowdhury MA. Advances in nanoparticles in targeted drug delivery–A review. Results in Surfaces and Interfaces. 2025;19:100529.
14. Zambonino MC, Quizhpe EM, Mouheb L, Rahman A, Agathos SN, Dahoumane SA. Biogenic Selenium Nanoparticles in Biomedical Sciences: Properties, Current Trends, Novel Opportunities and Emerging Challenges in Theranostic Nanomedicine. Nanomaterials. 2023;13(3):424.
15. Chen G, Yang F, Fan S, Jin H, Liao K, Li X, et al. Immunomodulatory roles of selenium nanoparticles: Novel arts for potential immunotherapy strategy development. Front Immunol. 2022;13.
16. Shahidin, Wang Y, Wu Y, Chen T, Wu X, Yuan W, et al. Selenium and Selenoproteins: Mechanisms, Health Functions, and Emerging Applications. Molecules. 2025;30(3):437.
17. Corbu VM, Gheorghe-Barbu I, Dumbravă AȘ, Vrâncianu CO, Șesan TE. Current Insights in Fungal Importance—A Comprehensive Review. Microorganisms. 2023;11(6):1384.
18. Serov DA, Khabatova VV, Vodeneev V, Li R, Gudkov SV. A Review of the Antibacterial, Fungicidal and Antiviral Properties of Selenium Nanoparticles. Materials. 2023;16(15):5363.
19. Ullah A, Mu J, Wang F, Chan MWH, Yin X, Liao Y, et al. Biogenic Selenium Nanoparticles and Their Anticancer Effects Pertaining to Probiotic Bacteria—A Review. Antioxidants. 2022;11(10):1916.
20. Madhavi A, Srinivasulu M, Shankar PC, Rangaswamy V. Synthesis and Applications of Fungal-Mediated Nanoparticles. Environmental and Microbial Biotechnology: Springer Nature Singapore; 2023. p. 113-131.
21. Ajadi AE, Ajijolakewu AK, Sorunke TA, Suleiman MM, Ayoola SA, Abdulai OO. Therapeutic Potential of Secondary Metabolites from Endophytic Fungi in Biotechnology and Medicine. Nigerian Journal of Pure and Applied Sciences. 2024:4887-4909.
22. El-Sayed E-SR, Abdelhakim HK, Ahmed AS. Solid-state fermentation for enhanced production of selenium nanoparticles by gamma-irradiated Monascus purpureus and their biological evaluation and photocatalytic activities. Bioprocess and Biosystems Engineering. 2020;43(5):797-809.

23. Gharieb MM, Soliman AM, Omara MS. Biosynthesis of selenium nanoparticles by potential endophytic fungi Penicillium citrinum and Rhizopus arrhizus: characterization and maximization. Biomass Conversion and Biorefinery. 2023;15(2):2319-2328.
24. Adeleke BS, Olowe OM, Ayilara MS, Fasusi OA, Omotayo OP, Fadiji AE, et al. Biosynthesis of nanoparticles using microorganisms: A focus on endophytic fungi. Heliyon. 2024;10(21):e39636.
25. Rathod S, Preetam S, Pandey C, Bera SP. Exploring synthesis and applications of green nanoparticles and the role of nanotechnology in wastewater treatment. Biotechnology Reports. 2024;41:e00830.
26. Sowmya R, Karthick Raja Namasivayam S, Krithika Shree S. A Critical Review on Nano-selenium Based Materials: Synthesis, Biomedicine Applications and Biocompatibility Assessment. Journal of Inorganic and Organometallic Polymers and Materials. 2024;34(7):3037-3055.
27. Hashem AH, Khalil AMA, Reyad AM, Salem SS. Biomedical Applications of Mycosynthesized Selenium Nanoparticles Using Penicillium expansum ATTC 36200. Biol Trace Elem Res. 2021;199(10):3998-4008.
28. Hussein HG, El-Sayed E-SR, Younis NA, Hamdy AEHA, Easa SM. Harnessing endophytic fungi for biosynthesis of selenium nanoparticles and exploring their bioactivities. AMB Express. 2022;12(1).
29. Saied E, Mekky AE, Al-Askar AA, Hagag AF, El-bana AA, Ashraf M, et al. Aspergillus terreus-Mediated Selenium Nanoparticles and Their Antimicrobial and Photocatalytic Activities. Crystals. 2023;13(3):450.
30. El-Sayed AIM, El-Sheekh MM, Abo-Neima SE. Mycosynthesis of selenium nanoparticles using Penicillium tardochrysogenum as a therapeutic agent and their combination with infrared irradiation against Ehrlich carcinoma. Sci Rep. 2024;14(1).
31. Sappapan R, Sommit D, Ngamrojanavanich N, Pengpreecha S, Wiyakrutta S, Sriubolmas N, et al. 11-Hydroxymonocerin from the Plant Endophytic Fungus Exserohilum rostratum. J Nat Prod. 2008;71(9):1657-1659.
32. Tan RX, Jensen PR, Williams PG, Fenical W. Isolation and Structure Assignments of Rostratins A–D, Cytotoxic Disulfides Produced by the Marine-Derived Fungus Exserohilum ostratum. J Nat Prod. 2004;67(8):1374-1382.
33. Greenfield M, Pareja R, Ortiz V, Gómez-Jiménez MI, Vega FE, Parsa S. A novel method to scale up fungal endophyte isolations. Biocontrol Sci Technol. 2015;25(10):1208-1212.
34. Ellis MB. Dematiaceous Hyphomycetes: CABI; 1971 1971/01.
35. Dunn M, Domsch KH, Gams W, Anderson T-H. Compendium of Soil Fungi. Taxon. 1982;31(3):600.
36. Morphology of Soil Fungi. Pictorial Atlas of Soil and Seed Fungi: CRC Press; 2002. p. 39-204.
37. Amin MA, Ismail MA, Badawy AA, Awad MA, Hamza MF, Awad MF, et al. The Potency of Fungal-Fabricated Selenium Nanoparticles to Improve the Growth Performance of Helianthus annuus L. and Control of Cutworm Agrotis ipsilon. Catalysts. 2021;11(12):1551.
38. Zhai X, Zhang C, Zhao G, Stoll S, Ren F, Leng X. Antioxidant capacities of the selenium nanoparticles stabilized by chitosan. Journal of Nanobiotechnology. 2017;15(1).
39. Varlamova EG, Goltyaev MV, Mal'tseva VN, Turovsky EA, Sarimov RM, Simakin AV, et al. Mechanisms of the Cytotoxic Effect of Selenium Nanoparticles in Different Human Cancer Cell Lines. Int J Mol Sci. 2021;22(15):7798.
40. Boroumand S, Safari M, Shaabani E, Shirzad M, Faridi-Majidi R. Selenium nanoparticles: synthesis, characterization and study of their cytotoxicity, antioxidant and antibacterial activity. Materials Research Express. 2019;6(8):0850d0858.
41. Olszowy-Tomczyk M. Synergistic, antagonistic and additive antioxidant effects in the binary mixtures. Phytochem Rev. 2020;19(1):63-103.
42. Rajasekar S, Kuppusamy S. Eco-Friendly Formulation of Selenium Nanoparticles and Its Functional Characterization against Breast Cancer and Normal Cells. J Cluster Sci. 2020;32(4):907-915.
43. Shin S, Saravanakumar K, Mariadoss AVA, Hu X, Sathiyaseelan A, Wang M-H. Functionalization of selenium nanoparticles using the methanolic extract of Cirsium setidens and its antibacterial, antioxidant, and cytotoxicity activities. Journal of Nanostructure in Chemistry. 2021;12(1):23-32.
44. Wadhwani S, Gorain M, Banerjee P, Shedbalkar U, Singh R, Kundu G, et al. Green synthesis of selenium nanoparticles using Acinetobacter sp. SW30: optimization, characterization and its anticancer activity in breast cancer cells. International Journal of Nanomedicine. 2017;Volume 12:6841-6855.
45. Islam SN, Naqvi SMA, Raza A, Jaiswal A, Singh AK, Dixit M, et al. Mycosynthesis of highly fluorescent selenium nanoparticles from Fusarium oxysporum, their antifungal activity against black fungus Aspergillus niger, and in-vivo biodistribution studies. 3 Biotech. 2022;12(11).
46. Anmol A, Jaiswal SK, Prakash R, Mihara H, Prakash NT. Concomitant synthesis and stabilization of selenium nanoparticles using extract of endophytic fungus, Nigrospora gullinensis. Research Square Platform LLC; 2022.
47. Kumar A, Prasad B, Manjhi J, Prasad KS. Antioxidant activity of selenium nanoparticles biosynthesized using a cell-free extract of Geobacillus. Toxicological and Environmental Chemistry. 2020;102(10):556-567.
48. Qian F, Li X, Tang L, Lai SK, Lu C, Lau SP. Selenium quantum dots: Preparation, structure, and properties. Appl Phys Lett. 2017;110(5).
49. Fouda A, Al-Otaibi WA, Saber T, AlMotwaa SM, Alshallash KS, Elhady M, et al. Antimicrobial, Antiviral, and In-Vitro Cytotoxicity and Mosquitocidal Activities of Portulaca oleracea-Based Green Synthesis of Selenium Nanoparticles. Journal of Functional Biomaterials. 2022;13(3):157.
50. Sowndarya P, Ramkumar G, Shivakumar MS. Green synthesis of selenium nanoparticles conjugated Clausena dentata plant leaf extract and their insecticidal potential against mosquito vectors. Artificial Cells, Nanomedicine, and Biotechnology. 2016;45(8):1490-1495.
51. Alagesan V, Venugopal S. Green Synthesis of Selenium Nanoparticle Using Leaves Extract of Withania somnifera and Its Biological Applications and Photocatalytic Activities. BioNanoScience. 2018;9(1):105-116.
52. Cole M. Method in plant biochemistry, volume 6: Assays for bioactivity. Phytochemistry. 1992;32(1):227.
53. Dumore NS, Mukhopadhyay M. Antioxidant properties of aqueous selenium nanoparticles (ASeNPs) and its catalysts activity for 1, 1-diphenyl-2-picrylhydrazyl (DPPH) reduction. J Mol Struct. 2020;1205:127637.
54. Khurana A, Tekula S, Saifi MA, Venkatesh P, Godugu C. Therapeutic applications of selenium nanoparticles. Biomedicine and Pharmacotherapy. 2019;111:802-812.
55. Karthik KK, Cheriyan BV, Rajeshkumar S, Gopalakrishnan M.

A review on selenium nanoparticles and their biomedical applications. Biomedical Technology. 2024;6:61-74.
56. An X, Yu W, Liu J, Tang D, Yang L, Chen X. Oxidative cell death in cancer: mechanisms and therapeutic opportunities. Cell Death and Disease. 2024;15(8).
57. Chuai H, Zhang S-Q, Bai H, Li J, Wang Y, Sun J, et al. Small molecule selenium-containing compounds: Recent development and therapeutic applications. Eur J Med Chem. 2021;223:113621.
58. Zhang H, Chen H, Guo G, Lin J, Chen X, Huang P, et al. Nanotechnology in prostate cancer: a bibliometric analysis from 2004 to 2023. Discover Oncology. 2025;16(1).
59. Ferro C, Florindo HF, Santos HA. Selenium Nanoparticles for Biomedical Applications: From Development and Characterization to Therapeutics. Advanced Healthcare Materials. 2021;10(16).
60. Ali BA, Allam RM, Hasanin MS, Hassabo AA. Biosynthesis of selenium nanoparticles as a potential therapeutic agent in breast cancer: G2/M arrest and apoptosis induction. Toxicology Reports. 2024;13:101792.
61. Hou J, Tamura Y, Lu H-Y, Takahashi Y, Kasugai S, Nakata H, et al. An In Vitro Evaluation of Selenium Nanoparticles on Osteoblastic Differentiation and Antimicrobial Properties against Porphyromonas gingivalis. Nanomaterials. 2022;12(11):1850.
62. Anastasiadi M, Polizzi K, Lambert RJW. An improved model for the analysis of combined antimicrobials: a replacement for the Chou-Talalay combination index method. J Appl Microbiol. 2017;124(1):97-107.
63. Xia Y, Xu T, Zhao M, Hua L, Chen Y, Wang C, et al. Delivery of Doxorubicin for Human Cervical Carcinoma Targeting Therapy by Folic Acid-Modified Selenium Nanoparticles. Int J Mol Sci. 2018;19(11):3582.
64. Spyridopoulou K, Aindelis G, Pappa A, Chlichlia K. Anticancer Activity of Biogenic Selenium Nanoparticles: Apoptotic and Immunogenic Cell Death Markers in Colon Cancer Cells. Cancers (Basel). 2021;13(21):5335.
65. Al-Duais MA, El Rabey HA, Mohammed GM, Al-Awthan YS, Althiyabi AS, Attia ES, et al. The anticancer activity of fucoidan coated selenium nanoparticles and curcumin nanoparticles against colorectal cancer lines. Sci Rep. 2025;15(1).
66. Zoidis E, Seremelis I, Kontopoulos N, Danezis G. Selenium-Dependent Antioxidant Enzymes: Actions and Properties of Selenoproteins. Antioxidants. 2018;7(5):66.
67. AlHasan L, Qi A, Al-Aboodi A, Rezk A, Shilton RR, Chan PPY, et al. Surface acoustic streaming in microfluidic system for rapid multicellular tumor spheroids generation. SPIE Proceedings; 2013/12/07: SPIE; 2013. p. 89235C.
68. Al-Abboodi A, Tjeung R, Doran P, Yeo L, Friend J, Chan P. Microfluidic chip containing porous gradient for chemotaxis study. SPIE Proceedings; 2011/12/21: SPIE; 2011. p. 82041H.
69. Rassami W, Soonwera M. In vitro pediculicidal activity of herbal shampoo base on Thai local plants against head louse (Pediculus humanus capitis De Geer). Parasitol Res. 2013;112(4):1411-1416.
70. Rabeea Banoon S, Younis Alfathi M, Shokouhi Mostafavi SK, Ghasemian A. Predominant genetic mutations leading to or predisposing diabetes progress: A Review. Bionatura. 2022;7(4):1-10.
71. Jabber Al-Saady MAA, Aldujaili NH, Rabeea Banoon S, Al-Abboodi A. Antimicrobial properties of nanoparticles in biofilms. Bionatura. 2022;7(4):1-9.
72. Al-Abboodi A, Mhouse Alsaady HA, Banoon SR, Al-Saady M. Conjugation strategies on functionalized iron oxide nanoparticles as a malaria vaccine delivery system. Bionatura. 2021;3(3):2009-2016.
73. Varlamova EG, Gudkov SV, Blinova EV, Blinov DS, Turovsky EA. Anticancer signal transduction pathways of selenium nanoparticles in mouse colorectal cancer model. Biochemical and Biophysical Research Communications. 2025;769:151962.
74. Puri A, Mohite P, Ansari Y, Mukerjee N, Alharbi HM, Upaganlawar A, et al. Plant-derived selenium nanoparticles: investigating unique morphologies, enhancing therapeutic uses, and leading the way in tailored medical treatments. Materials Advances. 2024;5(9):3602-3628.
75. Muhsin T, Hachim A. Antitumor and Antibacterial Efficacy of Mycofabricated Silver Nanoparticles by the Endophytic Fungus Papulaspora pallidula. American Journal of Bioengineering and Biotechnology. 2016.
76. Muhsin TM, Hachim AK. Mycosynthesis and characterization of silver nanoparticles and their activity against some human pathogenic bacteria. World J Microbiol Biotechnol. 2014;30(7):2081-2090.